



DESIGN DESCRIPTION

	Name and function	Date	Signature
Prepared by:	Stas Barabash, Co-PI Joakim Gimholt, EM		
Verified by:			
Approved by:			



ASPERA-3

Page left free intentionally



ASPERA-3

CHANGE RECORD

Version	Date	Changed Paragraphs	Remarks
Draft Revision 0	1999-03-30	All	New document
Draft Revision 1	1999-04-23	1.1, 1.7	MLI/Harness/DC/DC converter description added



ASPERA-3

Page left free intentionally



TABLE OF CONTENTS

1.	BRIEF EXPERIMENT DESCRIPTION	7
1.1	Experiment Hardware Description	7
1.2	The Neutral Particle Imager (NPI)	9
1.3	The Neutral Particle Detector (NPD).....	11
1.4	The Electron and Ion Spectrometer (EIS).....	17
1.5	The Ion Mass Analyser (IMA)	19
1.6	The Mechanical Scanner	21
1.7	The Digital Processing Unit (DPU).....	23



Page left free intentionally

1. BRIEF EXPERIMENT DESCRIPTION

1.1 Experiment Hardware Description

The ASPERA-3 instrument can be divided into four fundamental subunits; the mechanical scanner, the DPU including I/F-circuitry and three sensors; NPI (Neutral Particle Imager), NPD (Neutral Particle Detector) and ELS (ELectron Spectrometer) all together called the Main Unit and the ion mass analyzer (IMA). (See Figure 1.1, Figure 1.1.2 and Figure 1.1.3)

The mechanical scanner mechanically sweeps the instrument $\pm 90^\circ$ ($\pm 100^\circ$) to give the ASPERA-3 instrument a full 4π (unit sphere) coverage when the satellite is 3-axis stabilized. The scanner interfaces with the satellite mechanical interface through six mounting feet.

The DPU main task is to control the sensors and the mechanical scanner. The DPU will process, compress, store and forward the sensor data (and housekeeping data) to the satellite telemetry system. The DPU handles the commands sent to the ASPERA-3 instrument. The DPU includes interface circuitry to the sensors and the command/telemetry/power system of the satellite.

The Neutral Particle Imager (NPI), the Neutral Particle Detector (NPD), the Electron Spectrometer (ELS), mechanical scanner, Data Processing Unit (DPU) and the Ion Mass Analyser (IMA) are described in more detail below (Section 1.2. to 1.7).

The experiment is delivered with experimenter provided Multi Layer Isolation (MLI) blankets with an other layer of black Kapton (Indium-Tin-Oxide covered for low surface resistance) for the Main Unit sensor head and for the Ion Mass Analyser. Also provided is the interconnecting harness between the Main Unit and the Ion Mass Analyser. It should be noted that the S/C electrical interfaces only interfaces with then Main Unit DPU (cables routed through the scanner unit of ASPERA-3).

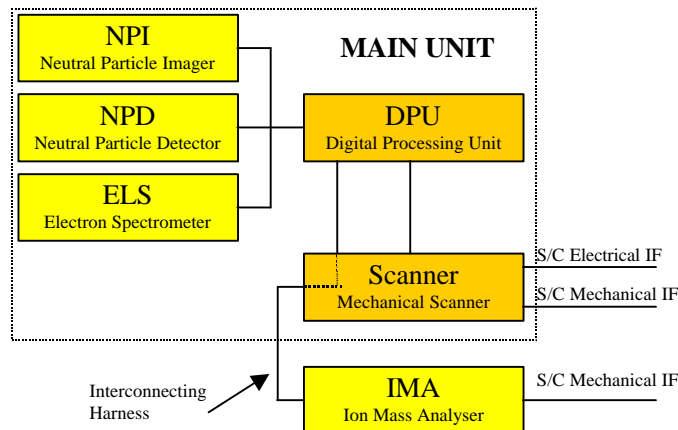


Figure 1.1-1 – Instrument hardware building blocks.

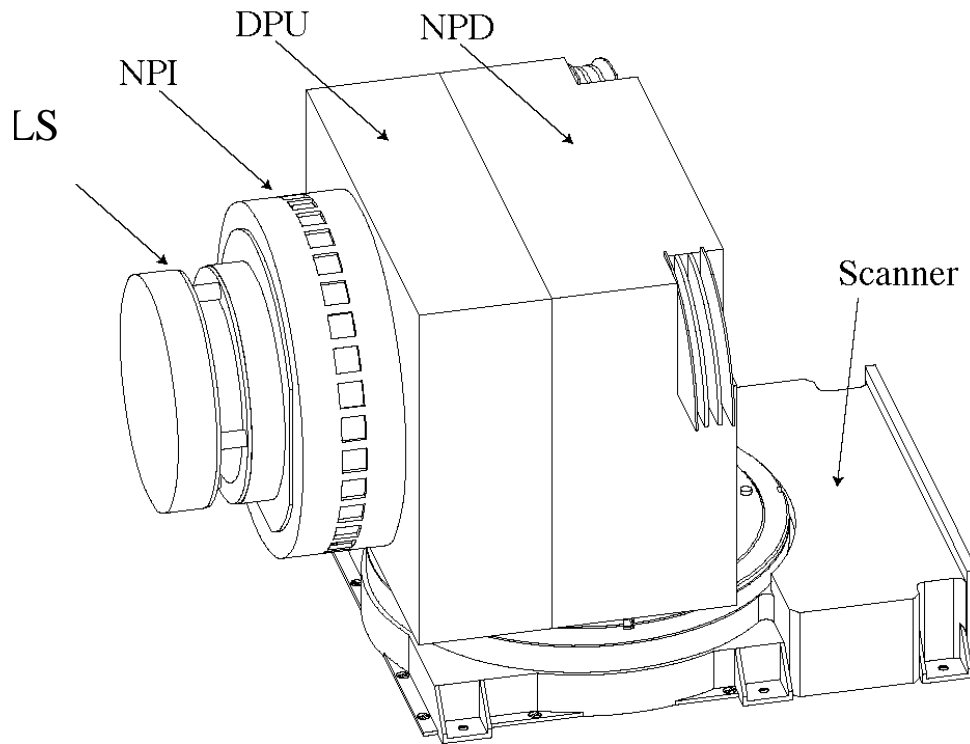


Figure 1.1.2 – The ASPERA-3 Main Unit

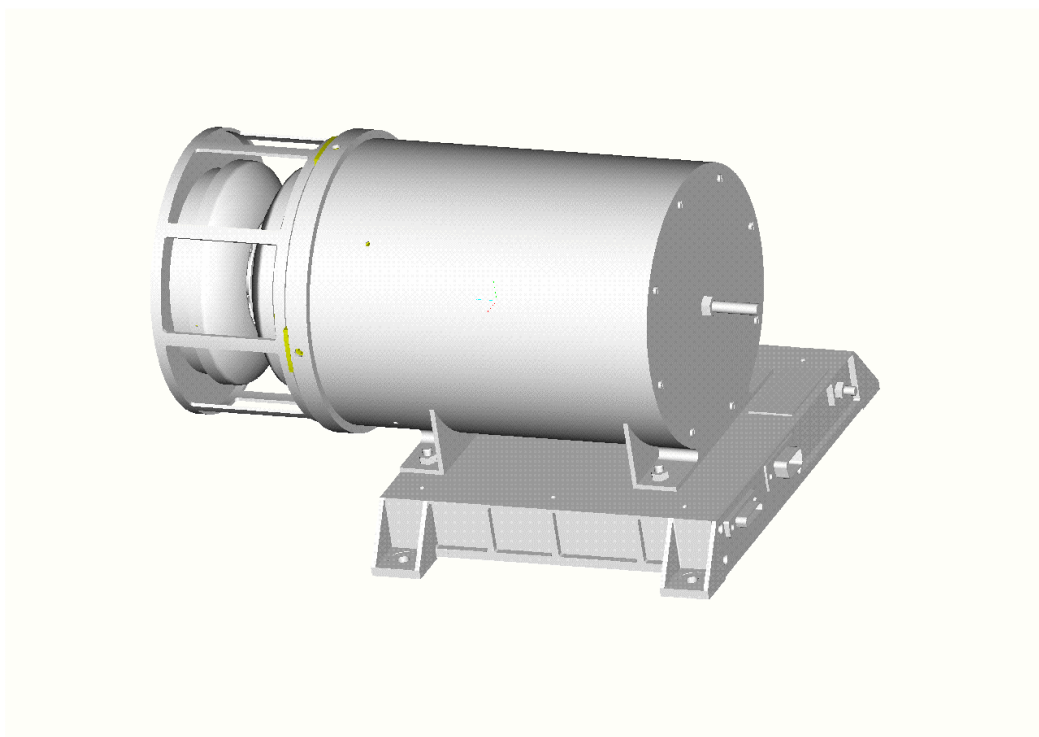


Figure 1.1.3 – The ASPERA-3 IMA Unit



Page left free intentionally

1.2 The Neutral Particle Imager (NPI)

The NPI (Neutral Particle Imager) head is a replica of the NPI - MCP sensor developed for the ASPERA-C experiment on the Mars-96 mission (Figure 1.2.1) and successfully flown on the Swedish micro satellite Astrid launched in 1995.



Figure 1.2.1 – *The low energy neutral particle imager for the ASPERA-C/Mars-96 experiment (spare unit)*

In the NPI the charged particles, electrons and ions, are removed by the electrostatic deflection system which consists of two disks separated by a 3 mm gap (Figures 1.2.2). The 5 kV potential between the grounded and biased disks results in a strong electric field which sweeps away all charged particles with energies up to 60 keV. Since the integral ENA flux substantially exceeds the charged particle flux for energies greater than 60 keV, this rejection energy is sufficient for satisfactory

performance. The disks also collimate the incoming beam in the elevation angle. Apart from being ON or OFF the deflection system can be operated in two other modes, alternative mode and sweeping mode. In the alternative mode, the deflection system is turned on and off for one sampling time. This mode will be used for more accurate separation between charged and neutral particles entering the system. In the sweeping mode, the deflection high voltage will be gradually swept from the maximum value to zero to provide approximate measurements of the plasma energy. The deflection system is connected to the high voltage supply via an optocoupler. Regulating the optocoupler reference voltage one can change the deflection voltage performing the sweeping and alternating. In order to reduce the time for discharging of the deflection system disks down to 1 ms, a second optocoupler is used.

The space between the deflection system disks is divided into 32 sectors by plastic spokes forming 32 azimuthal collimators with an aperture of $9^\circ \times 18^\circ$ each. Neutrals passing through the deflection system hit a 32 sided cone target with a grazing (20°) angle of incidence. The interaction with the target results in the secondary particle production, both electrons and ions, and / or reflection of the primary neutrals. The particles leaving the target block are detected by a MCP stack in the Z configuration with 32 anodes. The signal from the MCP gives the direction of the primary incoming neutral. The MCP operates in ion mode with a negative bias of -3.0 kV applied to the front side and thus detects (a) sputtered ions of the target material, (b) ions resulting from stripping of the primary neutrals, and (c) neutrals reflected from the target surface. In order to improve the angular resolution and collimate the particles leaving the interaction surface, 32 separating walls are attached to the target forming a star-like structure. This configuration allows the entering particles to experience multiple reflections and reach the MCP. NPI covers 4π in one instrument scan and produces an image of the ENA distribution in the form of an azimuth \times elevation matrix. The direction vector of 32 elements is read out once every 62.5 ms. Two sectors centered around the spin axis and looking toward the spacecraft body are blocked to provide monitoring of the MCP assembly dark counts. This space is also used for the ELS sensor harness.

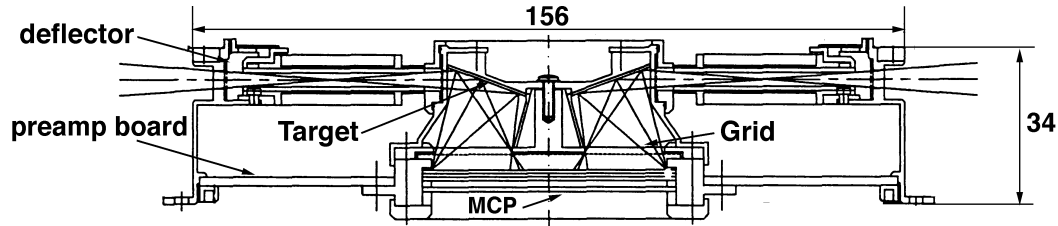


Figure 1.2.2 – *The NPI sensor cross section*

An important issue in the NPI design is a coating for the target which will suppress ever present flux of UV photons which enter the instrument and produce the UV background in the measurements. NPI uses the same coating as in the PIPPI and ASPERA-C experiments, namely, DAG 213, a resin - based graphite dispersion. This is similar to Aquadag which is a graphite dispersion in water. This coating demonstrated satisfactory performance in the PIPPI experiment flown in the Earth's magnetosphere.

NPI uses the 56 mm MCP plates manufactured at PHOTONIS, France and similar to the ones utilised in the PIPPI / ASTRID, ASPERA-C / Mars-96 experiments. The MOCAD preamplifiers (the same type as for the ICA experiment for the ESA Rosetta mission and IMA) are used. A summary of the instrument characteristics is given in Table 1.2.1.

Table 1.2.1 – *The NPI Sensor Characteristics*

Parameter	Value
Energy range	~0.1 - 60 keV
Energy resolution	No
Angular resolution (FWHM)	4.6° × 11.5°
Aperture per sensor	9° × 18°
Full field of view	9° × 344°
Azimuthal sectors	32
Geometrical factor	7.8×10 ⁻² cm ² sr
Geometrical factor per sector	2.5×10 ⁻³ cm ² sr
Efficiency	> 1 %
Power	0.8 W
Mass	0.7 kg

1.3 The Neutral Particle Detector (NPD)

The ASPERA-3 experiment utilises a combination of two sensors to perform comprehensive measurements of ENAs. The NPI sensor surveys ENA fluxes with sufficiently high angular resolution while the NPD sensor performs the velocity and mass measurements.

The NPD sensor consists of two identical detectors each of which is a pin-hole camera. Figure 1.3.1 provides a three-dimensional view of the two detectors along with an ENA trajectory.

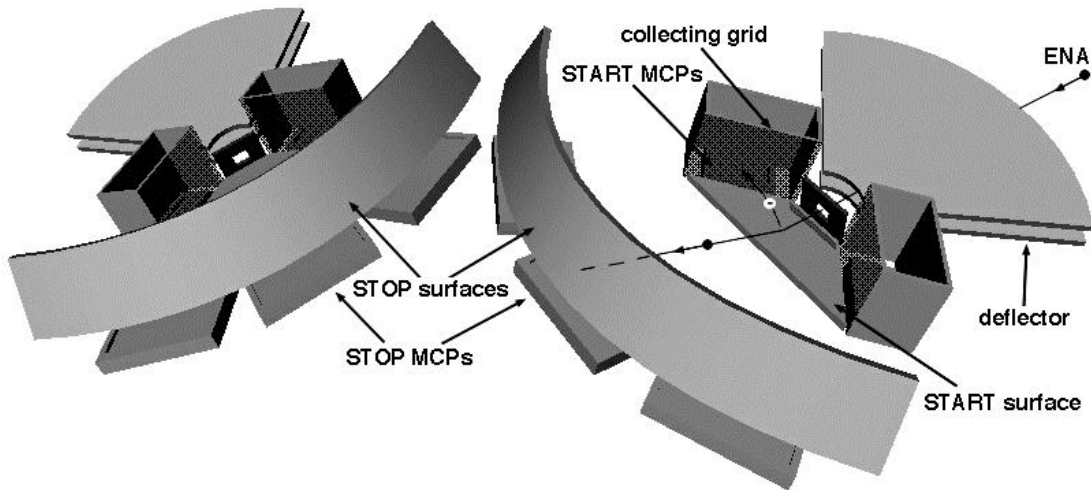


Figure 1.3.1 – *Three-dimensional view of the NPD principal components*

In each detector the charged particles, electrons and ions, are removed by the deflection system which consists of two 90° sectors separated by a 4.5 mm gap. In the normal operational mode the 8 kV potential (± 4 kV) applied to the disks and the resulting strong electric field sweeps away all charged particles with energies up to 70 keV. Apart from being ON or OFF the deflection system can be operated in the alternative mode. In this mode, the deflection system is turned on and off for one sampling time. This mode will be used for the more accurate separation between charged and neutral particles entering the system. The deflection system is connected to the high voltage supply via optocouplers. Regulating the optocoupler reference voltage one can change the deflection voltage performing. In order to reduce the time for discharging of the deflection system disks down to 1 ms, a second optocoupler is used for each deflection plate. The deflector also collimates the incoming beam in the elevation angle. The collimated ENA beam emerging from the 4.5×4.5 mm pin - hole hits the START surface under the grazing angle 20° and causes the secondary electron emission. By a system of collecting grids, the secondary electrons (SE) are transported to one of two MCP assemblies giving the START signal for the time-of-flight (TOF) electronics. The configuration of the START surface, START MCPs, and the collecting grids is shown in Figure 1.3.2 which also demonstrates the traced secondary electron trajectories. In this configuration, the MCP stack is located 7 mm above the START surface to minimise the flux of reflected photons which could reach the plates and increase the electron optic transmittance.

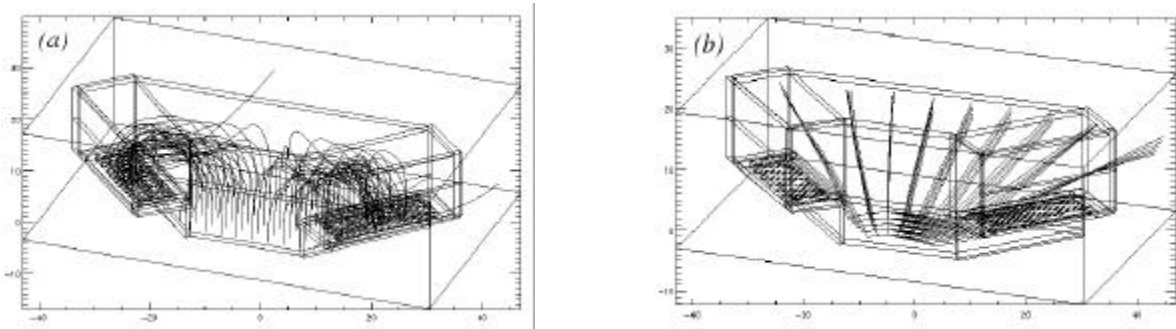


Figure 1.3.2 – The START surface with collecting grids and trajectories traced for (a) secondary electrons and (b) reflected 80 eV ions

The electric field created by the distributed potentials of collecting (+50V, +20V), repelling (-12V), and grounded grids as well as the MCP front side (+400 V) provides the collection of the secondary electrons onto the plates. Depending on the azimuth angle the collection efficiency varies from 60% to 90%. The incident ENAs are reflected from the START surface near-specularly. Since the charge state equilibrium is established during the interaction with the surface, the emerging beam contains both the neutral and ionised (positive and negative) components. To increase the total efficiency, no

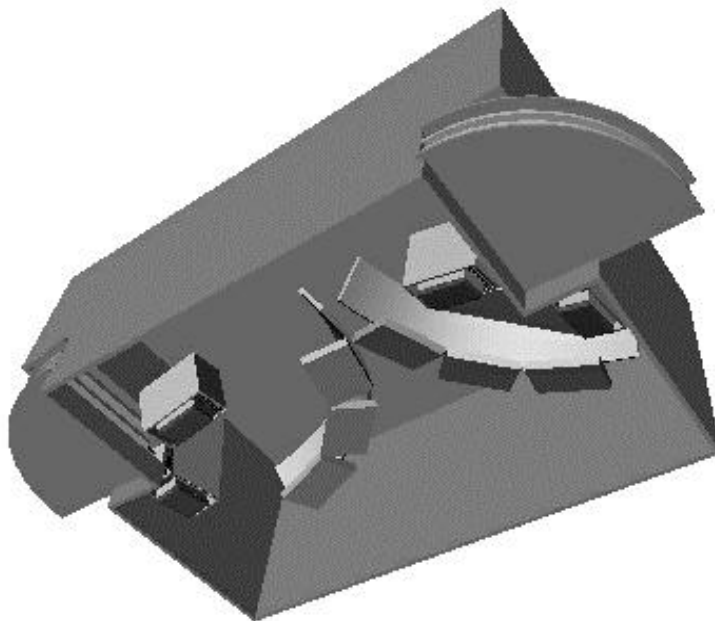


Figure 1.3.3 – Cut-away view of the Neutral Particle Detector (NPD sensor)

further separation by the charge is made. As proven by the ion tracing, there is very little disturbance to the reflected atomic ions leaving the START surface with an energy above 80 eV, introduced by the START electron optics. Therefore particles of all charge states - negative, neutral, and positive - will impact the second surface, the STOP surface, and again produce secondary electrons which are detected by one of the three MCP assemblies giving the STOP signal. The time of flight over the fixed distance of 8 cm defines the particle velocity. The STOP MCPs also give the azimuthal direction. Since the SE yield depends on mass for the same velocity, the pulse height distribution analysis of the START signals (the MCP charge) and independent analysis of the STOP signals provide the estimation of ENA mass. Each event is stored in the array START MCP charge × STOP MCP

charge × time-of-flight × direction. The array is accumulated over the sampling time 62.5 ms. Figure 1.3.3 shows a cut-away view of the NPD sensor.

The UV suppression in NPD is based on the START and STOP surface coatings and the coincidence of START / STOP signals. To increase the particle reflectivity, it is considered to use very smooth (roughness is of the order of 5 - 10 Å) START surfaces made of AL, Mg, or Cr. On the other hand the STOP surface is proposed to be made of sandblasted Al (roughness around 100 nm) covered by MgO. This combination has a very high secondary electron yield, low photoelectron yield and high UV absorption. However, the question regarding the acceptability of the highly UV

reflecting START surfaces will be addressed further in the laboratory studies. Both proposed surfaces are stable and do not require special maintaining. Table 1.3.1 gives the proposed surface characteristics for the hydrogen ENAs over the energy range 100 eV - 10 keV. The numbers are taken from literature and in some cases estimated or extrapolated. The numbers will be defined more exactly during development phase. Note, that grazing incidence on the START surface results in higher SE yields than normal incidence.

Table 1.3.1 – The START / STOP surface characteristics

Parameter	Value
SE yield for the START surface,	0.1 - 3
Particle reflection coefficient for the START surface,	0.1
Photoelectron yield (Lyman α) for the START surface,	0.001
UV reflection coefficient for the START surface,	0.1 - 1.0
SE yield for the STOP surface,	2 - 10
Photoelectron yield (Lyman α) for the STOP surface	0.001
UV reflection coefficient for the surrounding,	0.02
MCP efficiency for UV photons,	0.01
MCP efficiency for 200 eV electrons	0.6
START assembly collection efficiency	0.85
Collecting grid transmittance,	0.81

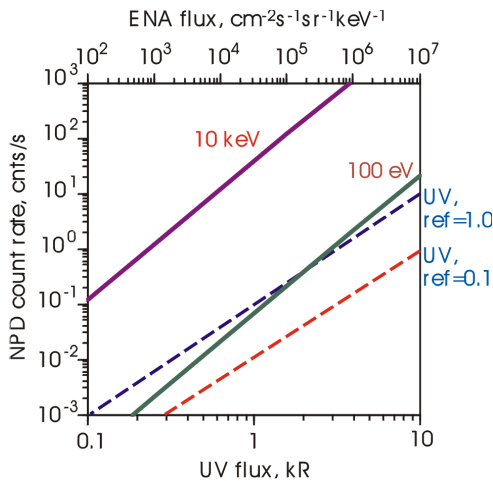


Figure 1.3.4 – The UV (Lyman α) background and hydrogen ENA count rates expected for the NPD minimum and maximum energies

Figure 1.3.4 presents the expected count rates calculated for the values from Table 1.3.1 for different ENA and UV fluxes (Lyman- α) and the TOF window 1.56 ms defined by the slowest (300 eV) oxygen atoms travelling the time-of-flight distance. The count rates corresponding to the Lyman- α radiation are given for two UV reflectivity coefficients of the START surface. The exact value will be defined in the laboratory tests.

The velocity resolution of the instrument is defined by three factors: geometrical path length variations in the TOF system ($\Delta L/L$), energy straggling during particle - START surface interaction ($\Delta E/E$), and timing errors ($\Delta T/T$). In order to estimate the first factor we have performed simulations of the NPD sensor geometry. The STOP surface shape was assumed to be spherical with a 8 cm radius around the START surface center and the 14° central angle. Figure 1.3.5 shows the matrix of the maximum $\Delta L/L$ values for each azimuth and elevation of incidence within the instrument's field of view for the specularly reflected particles. The average value is about 8% for the geometry in question.

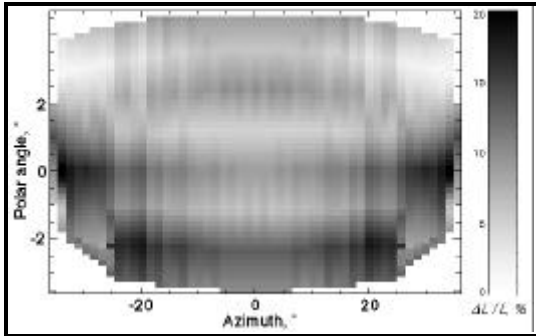


Figure 1.3.5 – The matrix of maximum path length variations for each azimuth and polar angle within the instrument's field of view

The timing error ΔT defined by the TOF electronics is negligible and the time of flight dispersion of the START / STOP electrons results in the relative timing error $\Delta T/T$ less than 8%. The spread in energy of the reflected ions does not exceed twice the energy loss due to the interaction process. The latter can be estimated to be less than 60% for energies less than 1 keV but increases with the ENA energy due to deeper penetration into the surface material. The exact value which will be defined by calibrations is expected to be less than 80%. The total velocity resolution given as the square root of the sum of the squared errors is about 40%, i.e., the energy resolution is 80% for a fixed mass.

The requirements for mass resolution are rather modest as compared to a typical plasma instrument. It is sufficient to resolve H and O only. Since the SE emission has a threshold of about 6×10^6 cm/s, the oxygen atoms can only be detected from about 300 eV. For the higher particle velocities, the differences in the SE yield for H and O reaches a factor of 2 for the same velocity. Using both START and STOP signals for the pulse - height analysis one can effectively increase this difference two times. Thus, an MCP assembly with a high pulse - height resolution (30 - 50%) is able to perform the hydrogen -oxygen mass identification.

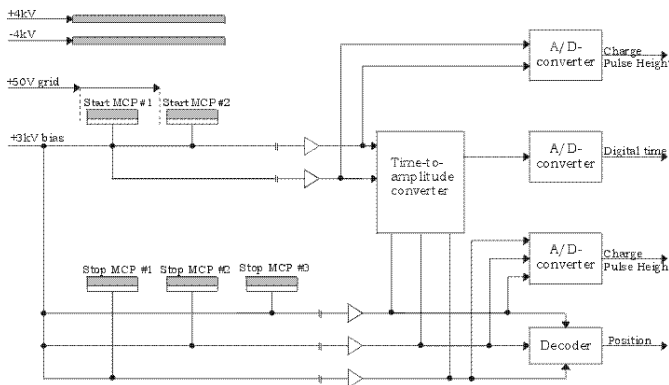


Figure 1.3.6 – The NPD electronics block diagram

The NPD sensor electronic block diagram is shown in Figure 1.3.6. The TOF electronics are based upon a novel, innovative design. They incorporate a flip-flop chain, with each cell having a fixed time-delay. The start signal from the Start-MCP will trigger the chain which will count up to the stop pulse.

The final count (TOF) is evaluated by digitally reading the flip-flop outputs. In order to minimise timing tolerance, the integrated LSI device will be fully temperature controlled. The system has already been developed and tested under contract from the MPAe at the University of Braunschweig (Germany). Radiation

total dose tests conducted at ESTEC proved the tolerance to be fully acceptable for space application. The entirely digital approach has considerable advantages over the standard analogue solutions. It provides a high resolution of 60 ps over a range of 6000 ns at a dissipating power of only 200 mW and a total mass of 60 grams (cf., 312 ps over 80 ns at 470 mW and 120 g for typical analogue systems). The system is easily reproducible. The maximum continuous event rate is greater than 150 kHz.

The output from each TOF channel is direction information (3 bits), the pulse-height analysed signals providing mass resolution (2×10 bits), and the TOF giving the energy spectral information (10 bits). This output will be further processed by the DPU.

Table 1.3.2 sums up the NPD characteristics.



Table 1.3.2 – The NPD Sensor Characteristics

Parameter	Value
Energy range	100 eV- 10 keV (H) 300 eV - < 100 keV (O)
Energy resolution (H)	0.8 (16 steps)
Mass resolution	H, O (8 steps)
Aperture per pixel	9° × 30°
Full field of view	9° × 180°
Azimuthal sectors	2 × 3
Geometrical factor	3.4×10^{-2} cm ² sr
Geometrical factor per pixel	6.2×10^{-3} cm ² sr (central) 5.3×10^{-3} cm ² sr (side)
Efficiency (H, 100 eV - 10 keV)	1 – 50%
Power	1.5 W
Mass	1.3 kg



Page left free intentionally

1.4 The Electron and Ion Spectrometer (EIS)

The Electron Spectrometer (ELS) sensor represents a new generation of ultra-light, low-power, electron sensor. It is formed by one spherical electrostatic analyzers top-hat and one collimator system. Particles enter the aperture at any angle in the plane of incidence. Electrons are then deflected into the spectrometer by applying a positive voltage to the inner spherical electron deflection plate. The electrons hit a micro channel plate (MCP) after being filtered in energy by the analyzer plates. The plates are stepped in voltage to achieve an energy spectrum. The hits are detected by preamplifiers connected to registers and the number of hits per sample interval are then further processed in the digital processing unit (DPU).

Electrons with energies up to 20 keV/q will be measured, with a maximum time resolution of one energy sweeps per four seconds. There are 16 anodes, each defining a 22.5° sector, behind the MCP each of which is connected to a preamplifier. The ELS sensor will be mounted on the ASPERA-3 scan platform, on top of the NPI sensor, in such a way that the full 4π angular distribution of electrons will be measured during each platform scan.

Table 1.4.1 – *The ELS instrument characteristics*

Parameter	Value
Mass	0.30 kg
Power	0.6 W
Dimensions	113 mm (diameter) x 36 mm (height)
Raw telemetry bit rate	8 kbps
Energy range	1 eV/q – 20 keV/q (in 128 steps)
Energy resolution ($\Delta E/E$)	7%
Acceptance angles	360° x 4°
Geometric factor	$7 \times 10^{-5} \text{ cm}^2 \text{ sr}$

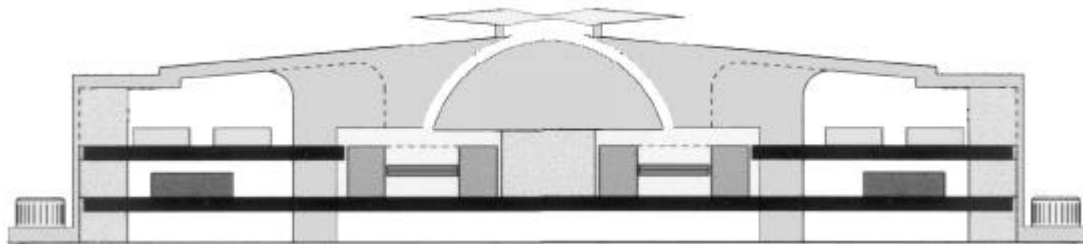


Figure 1.4.1 - *The ELS sensor.*

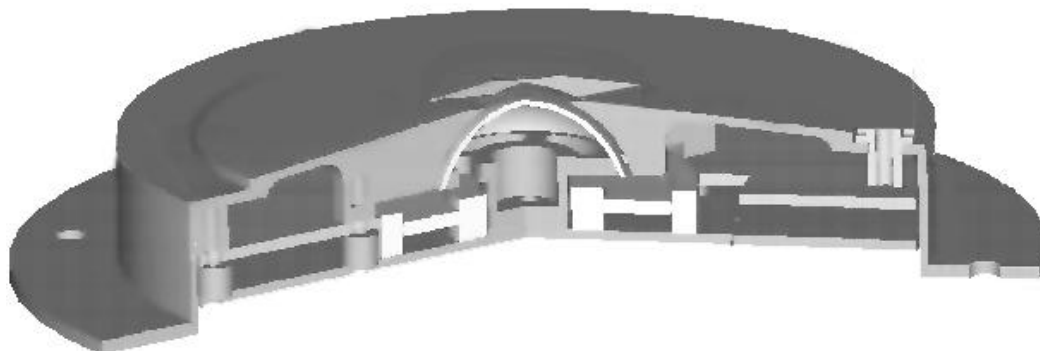


Figure 1.4.4.2 – *Cut-away view of ELS.*



ASPERA-3

Page left free intentionally

1.5 The Ion Mass Analyzer (IMA)

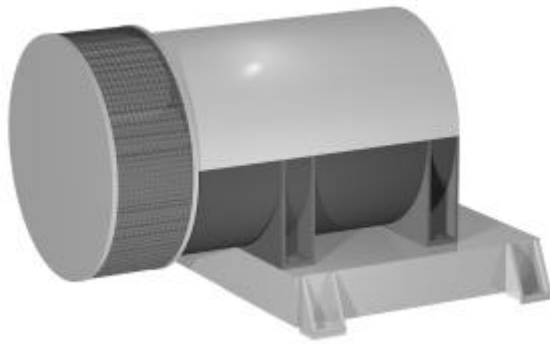
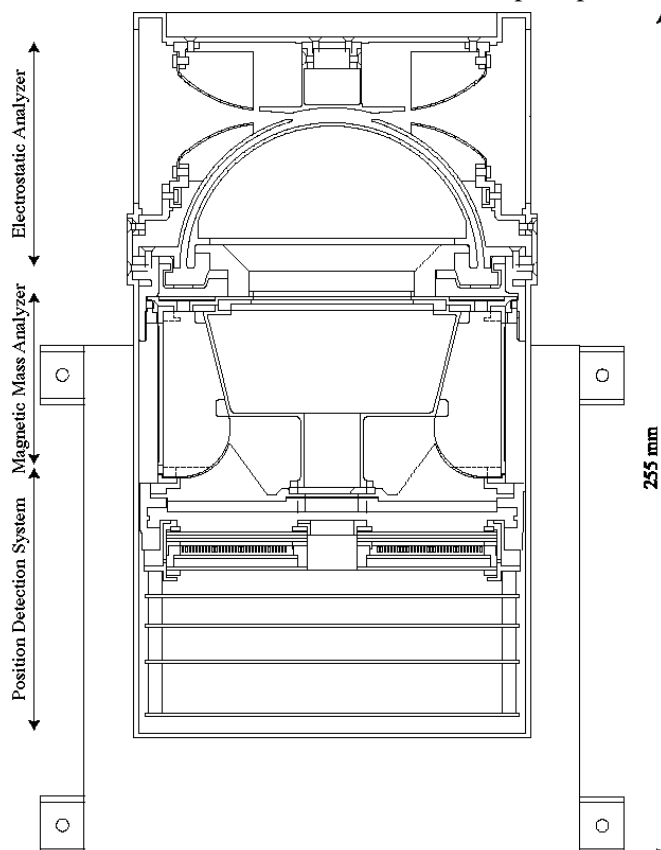


Figure 1.5.1 – *The Ion Mass Analyzer (IMA).*

The Ion Mass Analyzer (Figure 1.5.1 and 1.5.2.) is an improved version of the ion mass spectrographs TICS (Freja, 1992), IMIS (part of ASPERA-C, Mars-96, 1996), and IMI (Planet-B, 1998). It is an exact copy of the ICA instrument to be flown on Rosetta to comet Wirtanen in 2003. Particles enter the analyzer through an outer grounded grid. Behind the grid is a deflection system whose purpose is to deflect particles coming from angles lying between 45° and 135° with respect to the symmetry axis, into the electrostatic analyzer (ESA). Ions within a swept energy pass band will pass the ESA. The ions are then deflected in a cylindrical magnetic field set up by permanent magnets. The field deflects lighter ions more than heavy ions into the center of the analyzer. The ions finally hit a micro-channel plate (MCP) and are detected by an anode system. Ions are simultaneously analyzed regarding both direction and mass per charge. The magnet assembly can be biased with respect to the ESA to post-accelerate ions. This post-acceleration enables a selection of both mass range and mass resolution.

The electrons from the MCP are detected by an "imaging" anode system. A system of 32 concentric rings behind the MCP measures the radial impact position (representing ion mass), whereas 16 sector anodes measure the azimuthal impact position (representing ion entrance angle). In our



recent instrument on board Planet-B we used an analog detection system for impact location. For Rosetta and Mars Express we will employ a digital system which gives improved mass- and angular-resolution. Even with the analogue system, we have good mass resolution as shown in Figure 1.5.3. The mass detection technique utilized by IMA is ideal for the detection of ions of all masses (1 to $\sim 10^6$ a.m.u.), including sub-micron sized "dusty" plasma components, an unexplored plasma component believed to be of great importance in some cosmogonic scenarios. The characteristics of the IMA instrument are summarized in Table 1.5.1.

IMA will be an exact copy of the ICA instrument developed for Rosetta. The time schedule for the Mars Express mission would allow the fabrication, testing, and calibration of an additional unit in parallel with the fabrication of the two Rosetta flight models.

Figure 1.5.2 – *Cross section of IMA.*

Table 1.5.1 – IMA Characteristics

Parameter	Value
Mass	2.2 kg
Power	3.5 W (secondary)
Dimensions	255 x 150 x 150 (l x w x h)
Energy range	1 eV/q - 40 keV/q (in 128 steps)
Energy resolution	$\Delta E/E = 0.07$
Total field-of-view	$360^\circ \times 90^\circ$
Angular resolution	$22.5^\circ \times 4.5^\circ$
Geometric factor (per 22° sector)	$3.5 \times 10^{-4} \text{ (cm}^2 \text{ sr)}$

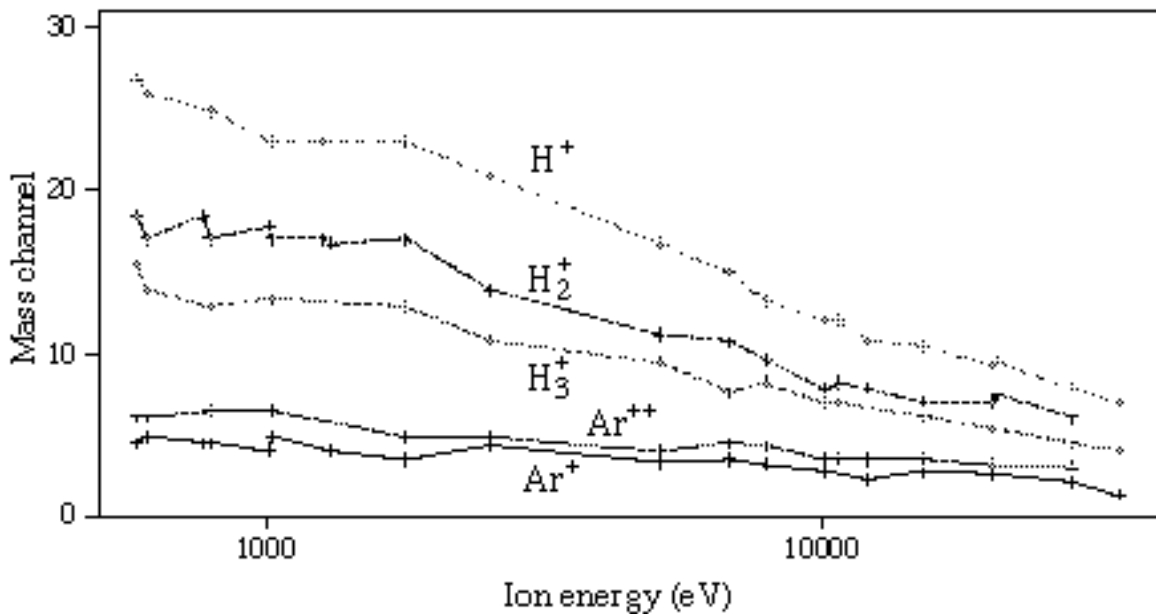


Figure 1.5.3 – Calibration results for the IMI instrument on board the Planet-B spacecraft.

In summary, the following unique features of IMA will contribute to the understanding of the Martian plasma environment:

- High angular resolution and 360° field of view, combined with the 90° entrance deflection system provides coverage of a large part of the unit sphere.
- Sufficient mass resolution and low "ghost" background for cold plasma (<1 keV).
- High dynamic range for fluxes, count rate dynamic range $>10^6$ counts per second.
- High sensitivity and good background immunity using the coincidence technique will eliminate the background to $<10^{-1}$ counts per second.

1.6 The Mechanical Scanner

The IRF ion and neutral particle imager instrument ASPERA-C, developed for the Russian Mars-96 project included a mechanical scanning and pointing platform. To obtain unit sphere (4π) coverage of the sensors, the platform was needed in order to move the sensor head within a 180 degree sector. The similar scanner (and usage) is going to be used as a platform for the ASPERA-3 instrument sensor assembly.

The platform interfaces the sensor head unit with the satellite mechanical and electrical subsystem, its main characteristics are:

- worm screw between two redundant stepper motors driving a large diameter worm wheel
- four small electronic boards for motor control and sensor interface
- two position sensors for determining positions 0 and 180 degrees and one for determination of intermediate angles
- feed-through cable loop with six cables and 6 connectors, each cable with 26 conductors (a maximum of 156 connections possible) interfacing through D-SUB or MDM connectors to the satellite electronic subsystem
- large diameter angular contact ball bearing
- housing and circular sensor platform manufactured in high-strength aluminum alloy

Table 1.6.1 – Mechanical scanner platform technical data

Technical data	Value	Unit
Maximum angle of rotation	+/-100	[deg.]
Angular movement per step, fs. Mode	0.0190	[deg.]
Angular movement per step, hs. Mode	0.0095	[deg.]
Angular position feedback resolution	0.05	[deg.]
Angular positioning accuracy	0.2	[deg.]
Operational rotation rate	1.5/3.0/6.0	[deg./s]
Maximum rotation rate	~25.0	[deg/s]
Power dissipation	0.5-2.0	[W]
Platform load	3.7	[kg]
Maximum platform load	~12	[kg]
Dimensions	44x200x273	[mm]
Mass	1.80	[kg]
Operational lifetime in vacuum	>3	[years]

A worm gear type of mechanism was selected in order to provide self-locking without electrical power, to minimize friction and to obtain a high gear ratio. The platform is made as a plug-in unit towards the sensor assembly. Great efforts have been spent to reduce mass, volume, power consumption and out-gassing in vacuum as well as to achieve high reliability. On command the platform can be turned to an arbitrary position or perform continuous scanning at any rate of rotation up to the maximum.



ASPERA-3

Page left free intentionally

1.7 The Digital Processing Unit (DPU)

The primary design drivers for the Digital Processing Unit (DPU) are optimum use of the allocated telemetry rate and correct handling of telecommands. The ASPERA-3 instrument will extensively use sophisticated loss-less data compression to enhance instrument scientific data yield. The basic algorithm used will be the compression technique based on “the Rice algorithm” (Universal Source Encoding for Space - USES) described in the CCSDS 111.0-W-2 (Consultative Committee for Space Data Systems) recommendation for data compression.

The ASPERA-3 DPU for the Mars Express mission will be based on the ICA (Ion Composition Analyzer) DPU for the ESA Rosetta mission. The ASPERA-3 DPU will be built by the same team at FMI that designs and manufactures the ICA DPU. The DPU comprise the following building blocks:

- THOR-II RISC processor running at <10MHz
- 128kB RAM (4pcs 32k x 8)
- 32kB PROM (4pcs 8k x 8)
- 512kB EEPROM (1pcs 512k x 8)
- 2MB mass memory (4pcs 512k x 8)
- ACTEL RH1020 and/or ACTEL RT1460
- Telemetry (TM) and telecommand (TC) drivers

Note: kB and MB above are used in the meaning “kilobinary” (kibi) and “Megabinary” (Mebi) if one follows the new IEEE-standard accepted in spring 1999.

The large memories (called mass memories) are used as telemetry buffer (FIFO style). The ACTEL RH1020 are used for telemetry and command interfaces (with drivers and receivers on S/C interfacing lines) and for internal address and data encoding and decoding. Figure 1.7.1 shows the DPU block diagram.

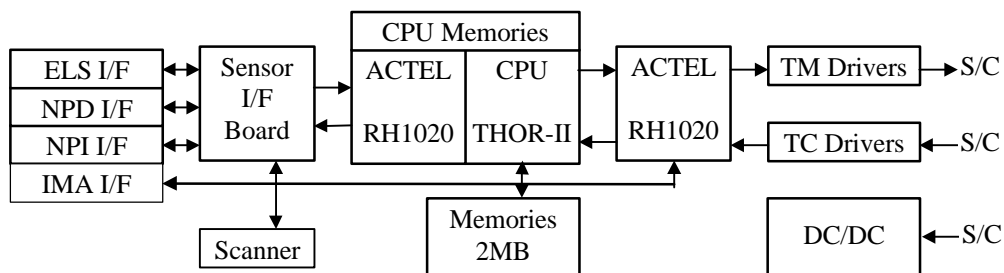


Figure 1.7-1 – Coarse DPU building blocks

Also included in the Main Unit DPU is the DC/DC converters interfacing with the S/C power system. The main characteristics of the Main Unit DC/DC converters are the following:

- Interpoint SMSA converters (isolated, level S, Interpoint class /KL)
- Generates regulated $\pm 5V$, $\pm 12V$ and $+30V$ from S/C provided $+28V$ (nom.)
- Generates maximum 5W per voltage
- Fully redundant (two independent converters)
- Input filtered to meet S/C EMC requirements
- Selection of main/redundant supply by HPC (High Power Commands) via relays



ASPERA-3

Page left free intentionally